

Double-diffusive natural convection in an inclined bi-L-shaped layered porous media: Darcy-Brinkman-Forcheimer model

A. Latreche and M. Djeddar*

Laboratory of Energetic Physics, Department of Physics, University Frères Mentouri Constantine 1, Algeria

*Corresponding author, email: mdjeddar@umc.edu.dz

Received date: June 09, 2018 ; accepted date: May 21, 2019

Abstract

In this study, Brinkman-Forchheimer-extended Darcy model of the two dimensional double diffusive natural convection heat and mass transfer generated in an inclined square bi-L-shaped layered porous cavity filled with Newtonian fluid has been investigated numerically. Each porous layer is considered isotropic, homogeneous and saturated with the same fluid. The cavity is heated and salted from below where as the vertical walls are assumed to be adiabatic and impermeable. The physical model for the momentum conservation equation makes use of the Darcy-Brinkman-Forcheimer model, and the set of coupled equations is solved using a finite volume approach. The power-law scheme is used to evaluate the flow, heat and mass fluxes across each of the control volume boundaries. Tridiagonal matrix algorithm with under-relaxation is used in conjunction with iterations to solve the nonlinear discretized equations. An in-house code developed for this study is validated using previous studies. The results are presented graphically in terms of streamlines, isotherms and iso-concentrations. In addition, the heat and mass transfer rate in the cavity is measured in terms of the average Nusselt and Sherwood numbers for various non dimensional parameters including, the buoyancy ratio N and the inclination angle α .

Keywords: Double-diffusive, Natural convection, Porous media, Darcy-Brinkman-Forcheimer model;

1. Introduction

Double-diffusive natural convection in a fluid-saturated porous medium is of significant interest to researchers owing to its various applications in different fields such as astrophysics, oceanography, chemical processes, geology, biology and geophysical problems. It also happens in many engineering applications such as the migration of moisture contained in fibrous insulation, drying processes, chemical transport in packed-bed reactors, grain storage installations, food processing, contamination transport in saturated soil, the underground disposal of nuclear wastes [1-6]. To have an overview of the phenomenon see some relevant fundamental works [7-9]. A very detailed summary of the work done in the past is presented by Nield and Bejan [10], Ingham and Pop [11], Vadász [12], Viskanta et al. [13] and Fernando [14]. Including different kinds of boundary conditions and methods of solutions, a literature review shows that relatively less attention has been given to the phenomenon of the double-diffusive natural convection in a porous multilayer cavity and most studies concerned with the thermosolutal convection in porous medium are made using a layer of porous medium [15-27], while in practice, several layers forming the structure of the porous medium. Hadidi et al. [28] studied numerically the double-diffusive convection in an inclined rectangular collector filled with two parallel porous layers.

Each porous layer is considered homogeneous, isotropic and saturated with the same fluid. The vertical walls of porous cavity are subjected to uniform temperature and concentration whereas the other surfaces are adiabatic and impermeable. They considered the case of mainly concentration driven flow ($N = 10$). They used a scale analysis to characterize the effect of the permeability ratio on the heat and mass transfer. The study showed that the permeability of the two porous layers has significant effect on the flow structure and transfers and indicated the existence of three regimes, namely, a diffusive regime low values of permeability ratio, a transition regime where mean Nu and Sh numbers increase with an increase of permeability ratio and an asymptotic regime where Nu and Sh become independent of permeability ratio. They also analyzed and discussed the effects of inclination angle on heat and mass transfers. Two-dimensional thermosolutal natural convective heat and mass transfer in a bi-layered and inclined porous enclosure has been studied by same authors [29]. All porous layers-cavity may occupy different positions relative to the horizontal axis for inclination angle values from 0° to 60° . A scale analysis for predicting mass transfer rate is represented for the case, where the two porous layers in the cavity are arranged vertically and for solute-driven flows ($N \gg 1$). The numerical results showed the existence of the optimal angle of inclination value that leads to a maximum heat and mass transfers. Baytas et al. [30] presented a

numerical study on double diffusive natural convection in another geometrical multilayer; a saturated porous layer and an overlying fluid layer in an enclosure using the non-Darcy flow model. The problem has been investigated for two cases; namely case I where the interface between fluid and porous layer is horizontal, and case II where the interface contains a step that has a height a . The fluid flow and heat and mass transfer has been investigated for different values of the step height and the Rayleigh and Darcy numbers. The results show that the height of the step at the interface has a significant effect on the flow field and heat and mass transfer from the left-hand to the right-hand walls in the composite enclosure. Double diffusive convection in a vertical enclosure inserted with two saturated porous layers confining a fluid layer has been analyzed by Bennacer et al. [31], the effect of hydraulic anisotropy on the rate of heat and mass transfer is discussed. It is found that the rate of heat transfer and the rate of mass transfer are weak functions of the Darcy number for high and low permeability regimes. For a certain range of the parameters, the rate of heat transfer decreases when the flow penetrates into the porous layer. Hence, there is an optimum (minimum) value of Nusselt number, which is a function of the anisotropy parameter.

To our knowledge no work is cited in an inclined bi-L-shaped layered porous media which is subject of this work.

2. Mathematical modeling

Consider steady two-dimensional natural convection in an inclined square cavity of side H . The cavity contains two porous L-shaped layers; each one is considered isotropic, homogeneous with constant thermo physical properties and saturated with the same fluid. All the walls are impermeable. Two opposing walls of the cavity are adiabatic and the other two walls are maintained at fixed different temperatures and concentrations as depicted in Figure 1. Hypotheses of incompressible and laminar flow are considered and the interaction between the thermal and concentration gradients, (Soret and Dufour effects) are neglected. The flow is driven by combined buoyancy forces because of both temperature as well as concentration variations. So the density is taken as a function of both temperature and concentration levels through the Boussinesq approximations:

$$\rho = \rho_0 [1 - \beta_T (T - T_l) - \beta_S (S - S_l)] \quad (1)$$

Where:

$$\beta_T = -\frac{1}{\rho_0} \left(\frac{\partial \rho}{\partial T} \right)_{P,S}$$

coefficient.

$$\beta_S = -\frac{1}{\rho_0} \left(\frac{\partial \rho}{\partial S} \right)_{P,T}$$

is the concentration expansion coefficient.

The model considered is the Darcy -Brinkman-Forcheimer. Under the above assumptions, the dimensionless equations for conservation of mass, momentum, energy and Species transport are given by:

$$\frac{\partial u}{\partial x} + \frac{\partial v}{\partial y} = 0 \quad (2)$$

$$\begin{aligned} \varepsilon_i \frac{\partial u}{\partial t} + u \frac{\partial u}{\partial x} + v \frac{\partial u}{\partial y} = -\frac{\partial P}{\partial x} - \frac{P_r}{Da_i} \varepsilon_i^2 u - \\ 1.75 \sqrt{\frac{\varepsilon_i (u^2 + v^2)}{150 Da_i}} u + Pr \varepsilon_i^2 \left(\frac{\partial^2 u}{\partial x^2} + \frac{\partial^2 u}{\partial y^2} \right) + \\ Ra Pr \varepsilon_i^2 (T + NS) \sin \alpha \end{aligned} \quad (3)$$

$$\begin{aligned} \varepsilon_i \frac{\partial v}{\partial t} + u \frac{\partial v}{\partial x} + v \frac{\partial v}{\partial y} = -\frac{\partial P}{\partial y} - \frac{P_r}{Da_i} \varepsilon_i^2 v - \\ 1.75 \sqrt{\frac{\varepsilon_i (u^2 + v^2)}{150 Da_i}} v + Pr \varepsilon_i^2 \left(\frac{\partial^2 v}{\partial x^2} + \frac{\partial^2 v}{\partial y^2} \right) + \\ Ra Pr \varepsilon_i^2 (T + NS) \cos \alpha \end{aligned} \quad (4)$$

$$\sigma_i \frac{\partial T}{\partial t} + u \frac{\partial T}{\partial x} + v \frac{\partial T}{\partial y} = \left(\frac{\partial^2 T}{\partial x^2} + \frac{\partial^2 T}{\partial y^2} \right) \quad (5)$$

$$\varepsilon_i \frac{\partial S}{\partial t} + u \frac{\partial S}{\partial x} + v \frac{\partial S}{\partial y} = \frac{1}{Le} \left(\frac{\partial^2 S}{\partial x^2} + \frac{\partial^2 S}{\partial y^2} \right) \quad (6)$$

The subscript $i=1, 2$ denoting the respective sub layers. Where the dimensionless variables are:

$$\begin{aligned} x = \frac{X}{H}, y = \frac{Y}{H}, u = \frac{U}{a/H}, v = \frac{V}{a/H}, T = \frac{T - T_l}{T_h - T_l}, \\ S = \frac{S - S_l}{S_h - S_l}, P = \frac{\varepsilon^2 H^2}{\rho_0 a^2} P, t = \frac{a}{H^2} t \end{aligned} \quad (7)$$

The dimensionless boundary conditions are:

$$\forall x : \begin{cases} y = 0 : T = S = 1, u = v = 0 \\ y = 1 : T = S = 0, u = v = 0 \end{cases} \quad (8)$$

$$\forall y : x = 0 \text{ or } 1 : \frac{\partial T}{\partial x} = \frac{\partial S}{\partial x} = u = v = 0 \quad (9)$$

At the interface between the two layers, the appropriate conditions of the variable and fluxes continuity can be written as:

$$\left. \begin{aligned} x = \frac{1}{3}, \quad \frac{1}{2} < y < 1 \\ x = \frac{2}{3}, \quad 0 < y \leq \frac{1}{2} \end{aligned} \right\} \phi_1 = \phi_2 \quad (10)$$

Where ϕ may correspond to P, u, v, T and S .

The average values of Nusselt and Sherwood numbers evaluated on the bottom wall are given by:

$$Nu = -\int_0^1 \frac{\partial T}{\partial y} dx \Big|_{y=0}, Sh = -\int_0^1 \frac{\partial S}{\partial y} dx \Big|_{y=0} \quad (11)$$

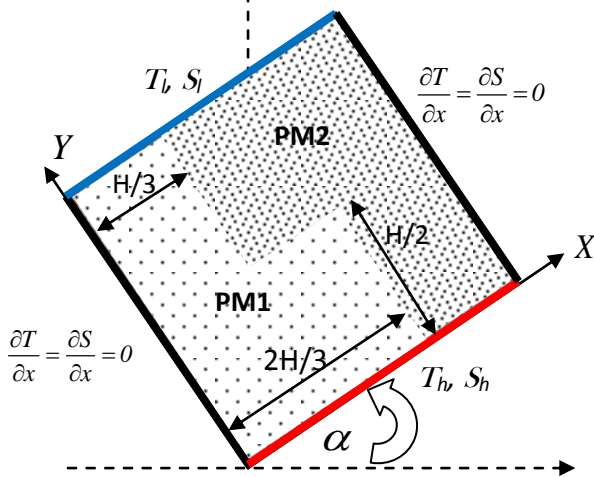


Figure 1. Physical Model and Geometry

3. Numerical solution

The volume finite method described by Patankar [32] is employed to solve numerically the governing equations together with the boundary conditions. The power-law scheme is used to evaluate the convective terms. The system of nonlinear discretized equations is solved iteratively by means of the Tridiagonal matrix algorithm with under-relaxation. The computation domain is divided into rectangular control volumes with one grid located at the centre of the control volume that forms a basic cell.

The set of conservation equations are integrated over the control volumes, leading to a balance equation for the fluxes at the interface.

The steady state was considered to have been reached at when the changes in u, v, T and S satisfies the equation:

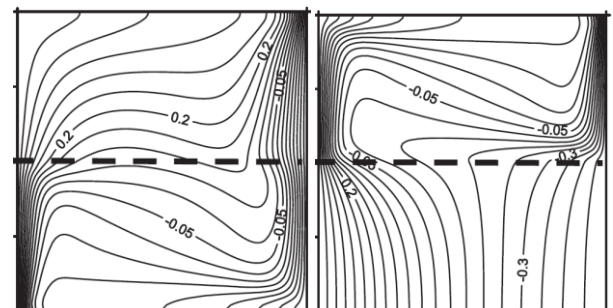
$$\frac{\sum_i \sum_j (\phi_{i,j}^{new} - \phi_{i,j}^{old})}{\sum_i \sum_j \phi_{i,j}^{new}} \leq 10^{-6} \quad (12)$$

Where the subscripts i and j denote grid locations in the (x, y) plane. A further decrease of the convergence criteria 10^{-6} does not cause any significant change in the final results. Numerical tests, using various mesh sizes, were done for the same conditions in order to determine the best compromise between accuracy of the results and computer time. A mesh size of 62×62 was adopted.

The accuracy of the in-house code was checked using previous studies. Table 1 presents comparisons for the natural heat transfer in an inclined porous cavity for four different inclination angles. Figure 2 presents comparisons for the double-diffusive natural convection in a bi-layered and inclined porous cavity. The results given here are in good agreement with the previous studies.

Table 1: Comparison of average Nusselt Number with α for Darcy model for $Ra^* = 100, A = 2$

$\alpha(^{\circ})$	Nu			
	Ref.[33]	Ref.[21]	Ref.[34]	Present work
0	2.46	2.59	2.65	2.58
5	2.53	2.60	2.64	2.65
10	2.55	2.24	2.60	2.68
15	2.39	2.39	2.44	2.47



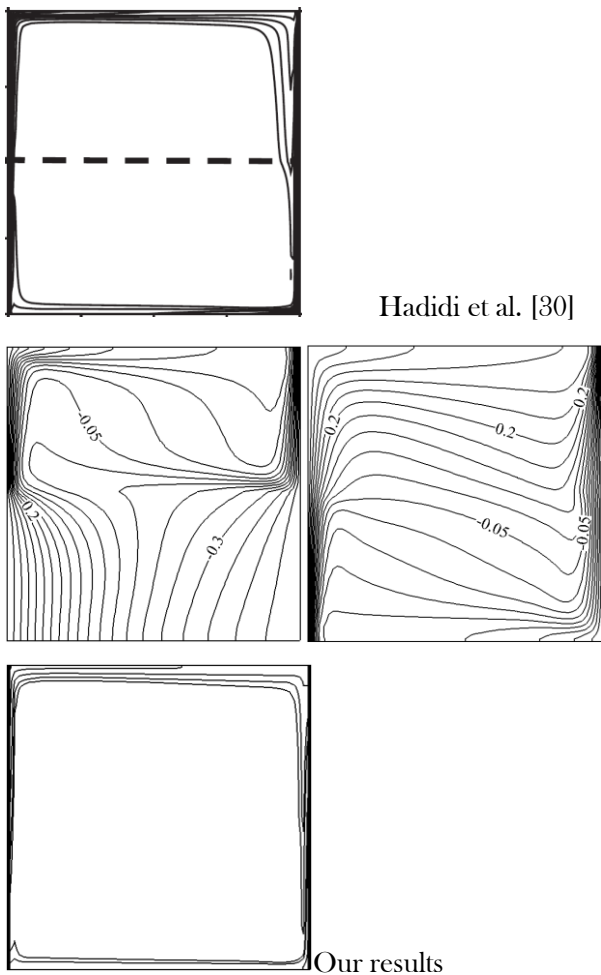


Figure 2. Comparison of isotherms (left for $Da_1=10^{-6}$, $Da_2=10^{-3}$ and right $Da_1=10^{-3}$, $Da_2=10^{-4}$), and iso-concentration lines ($Da_1=10^{-3}$, $Da_2=10^{-4}$) for $\epsilon_1=0.4$, $\epsilon_2=0.5$, $Ra=7 \cdot 10^6$, $\alpha=60^\circ$, $Pr=7$, $Le=100$ and $N=3$ with Hadidi et al. [30] work.

4. Results and discussion

4.1. Considered situations

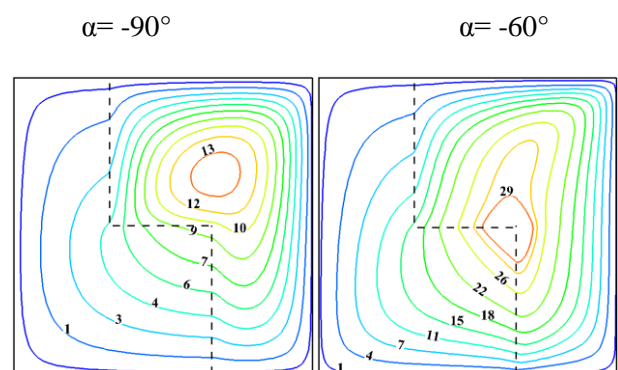
In the present work, the results are displayed in the form of stream, iso-thermal and iso-concentration lines to investigate the effect of inclination angle ($-90^\circ \leq \alpha \leq 90^\circ$), buoyancy ratio ($-5 \leq N \leq 5$), while Rayleigh, Lewis and Prandtl numbers are taken as $5 \cdot 10^6$, 0.1 and 4.5 respectively. The porosity and the Darcy number of the 2 layers are $\epsilon_1=0.6$, $\epsilon_2=0.4$, $Da_1=10^{-5}$ and $Da_2=10^{-4}$. The rate of heat and mass transfer at different conditions in the cavity is measured in terms of the average Nusselt number and the average Sherwood number.

4.2. Flow, isotherms and iso-concentrations distributions

Extensive parametric study has been done to delineate the flow, heat and solute transport mechanism.

To show the effects of the angle of inclination (α), stream lines, isotherms and iso-concentration lines are presented in Figure 3-5 and Figure 6-8 for $N=-5$ and 3 respectively.

For the opposed flow ($N=-5$) and for non-inclined enclosure ($\alpha=0^\circ$), flow lines (Figure 3) are split into two distinct cells. The big one covers the majority portion of cavity where the flow is counter-clockwise and ψ_{max} is about four times higher than that of the second cell which sits at the top right of the cavity where the flow is clockwise. This second cell disappears once the cavity tilts clockwise ($-90^\circ < \alpha < 0^\circ$) and the vortex strength of the fluid in the porous medium increases by the increase of the inclination angle until 75° where ψ_{max} reaches a maximum value. A significant first layer flow resistance is noticeable; this behavior is due to the low permeability of the first porous layer. For this purpose, the fluid circulation in the second porous layer is more favorable and the thermo-solutal convection is more pronounced in this layer. The same behavior we can see when the cavity is counter-clockwise tilted ($0^\circ < \alpha < 90^\circ$) with a difference that as α increases the size and the intensity of the first cell decrease in favor of the second one. For isotherm lines, it can be seen in Figure 4 that the isotherms are more distorted when inclination increases. The thermal boundary layer develops near the lower part first layer wall and near the upper part second layer wall when the cavity is clockwise tilted, and vice versa when the cavity is counter-clockwise tilted (near the upper part first layer wall and near the lower part second layer wall). For iso-concentration lines, it can be seen in Figure 5 that at small values of the inclination angle the iso-concentrations are almost parallel to the active walls, indicating that the mass transfer tend to a diffusive situation. The iso-concentration lines are more and more distorted in both layers when inclination increases.



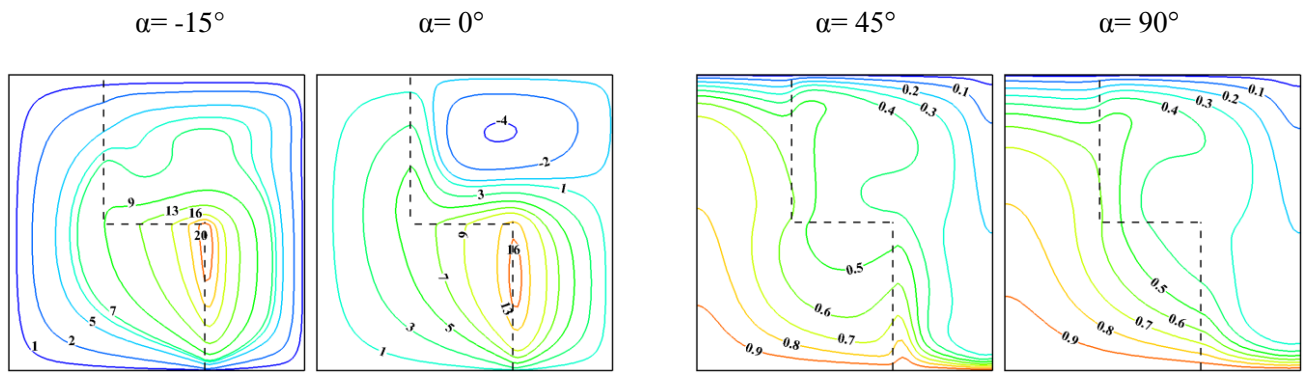


Figure 4. Isotherms for different α for $N = -5$.

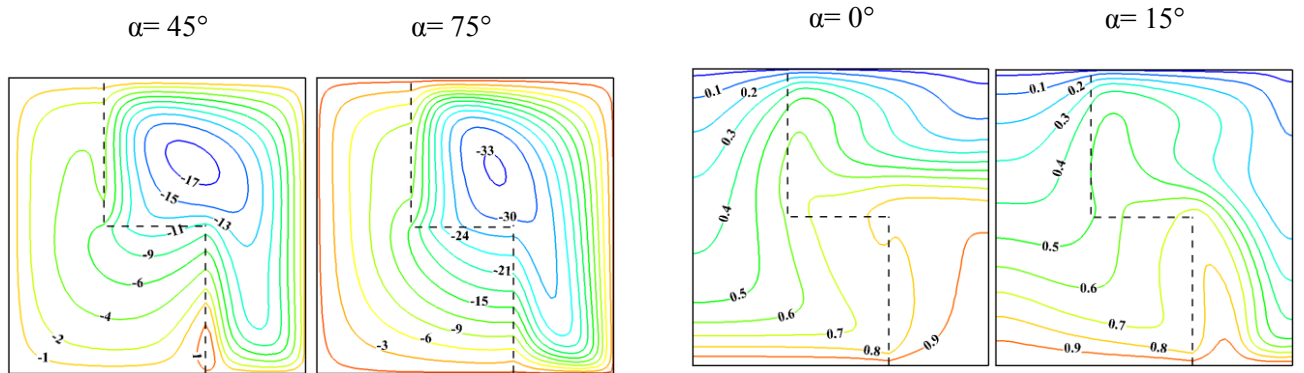
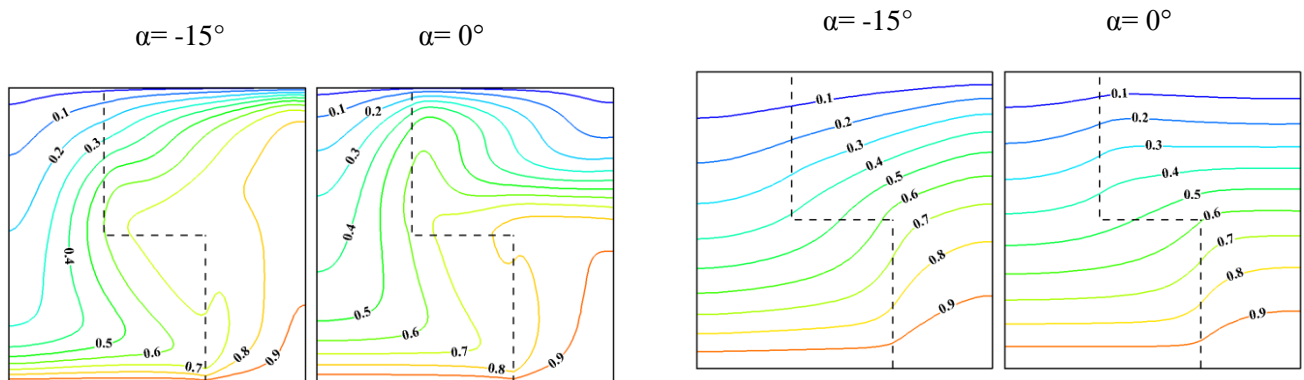
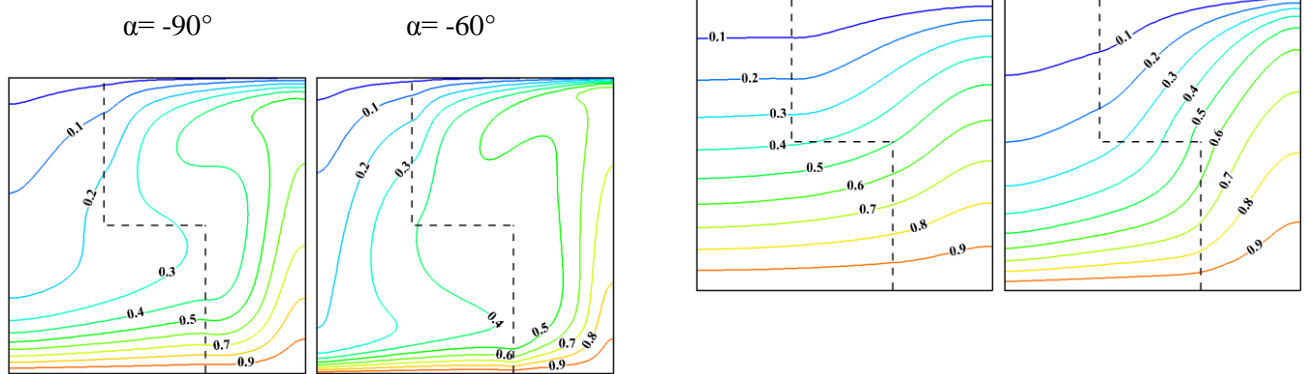


Figure 3. Streamlines for different α for $N = -5$.



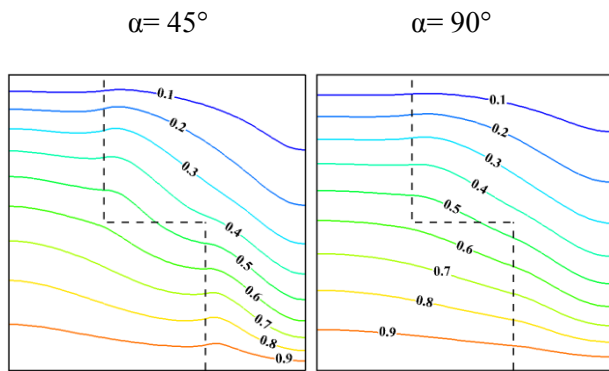


Figure 5. Iso-concentrations for different α for $N = -5$.

The same behaviors of the opposed flow we can see for the assisting flow case ($N=3$) with some variations, the flow is mono-cellular (Figure 6) when the cavity tilts clockwise, and multi-cellular (the second cell appears at the bottom right of the second layer) when the cavity is counter-clockwise tilted until 45° where the flow becomes mono-cellular and the vortex strength of the fluid is at the maximum. The thermal boundary layer appears for lower angle of inclination near the left lower second layer wall and it develops near the right of the lower second layer wall and near the upper part first layer wall when the cavity is clockwise tilted, and vice versa when the cavity is counter-clockwise tilted (Figure 7). For iso-concentration lines, it can be seen in (Figure 8) that the iso-concentrations are more and more distorted in both layers in comparison with the opposed flow especially for low angle of inclination. Indeed, the thermo-solutal convection is well pronounced in the two layers.

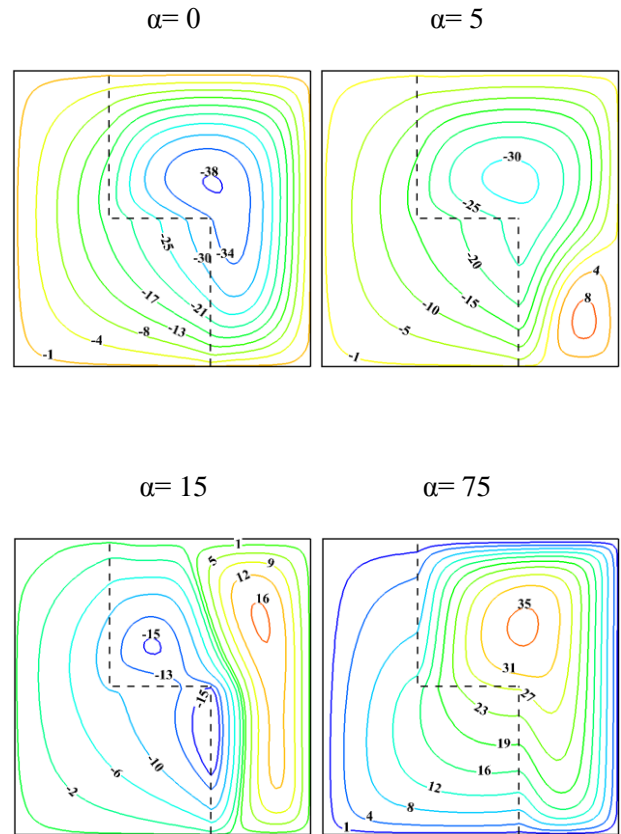
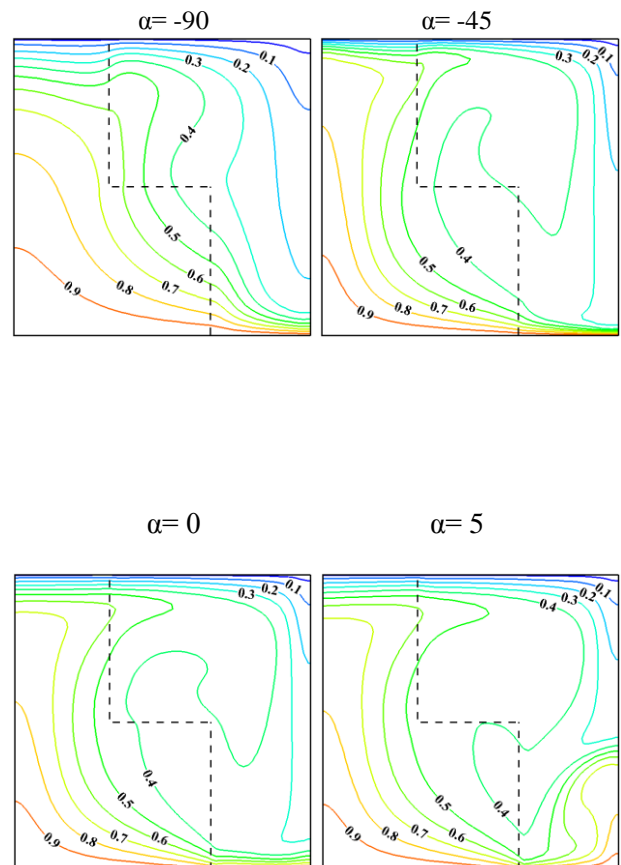
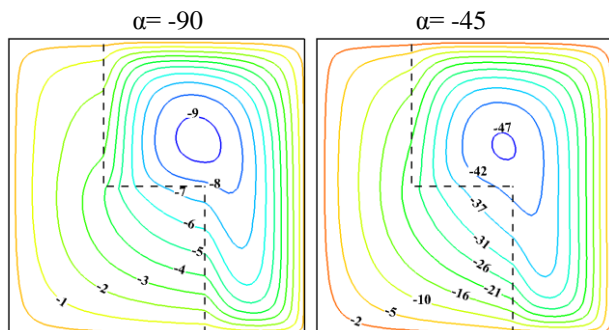


Figure 6. Streamlines for different α for $N = 3$.



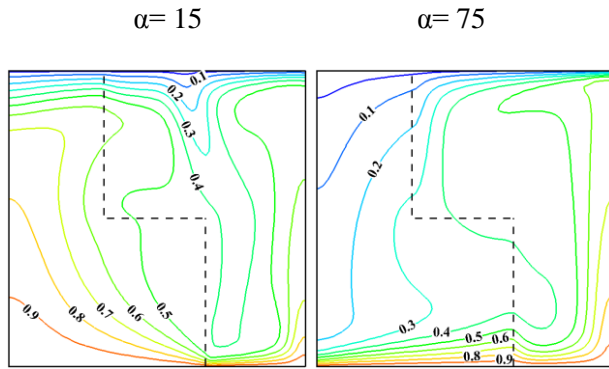


Figure 7. Isotherms for different α for $N=3$.

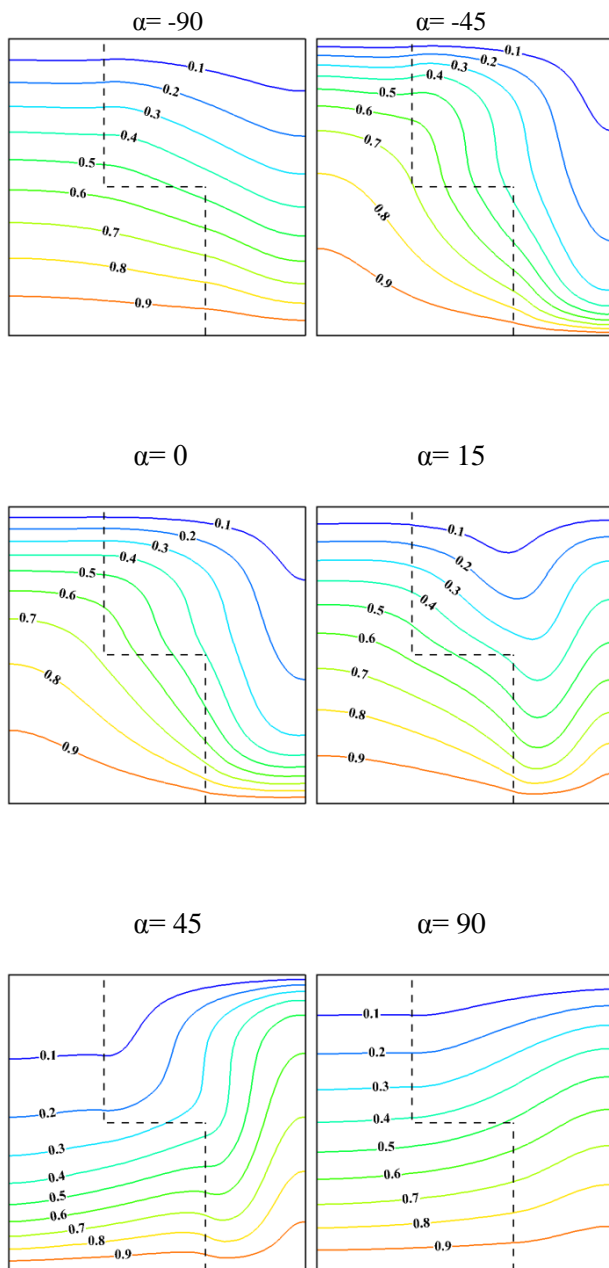


Figure 8. Iso-concentrations for different α for $N=3$.

The effects of the buoyancy ratio N on streamlines are presented in (Figure 9) for tilted angle $\alpha=15^\circ$. Flow lines are split into two distinct cells for all values of N excepting $N=-1$ where the flow is mono-cellular, the vortex strength of the fluid in the porous medium increases by the increase of the buoyancy ratio whether it flow opposed or cooperating cases.

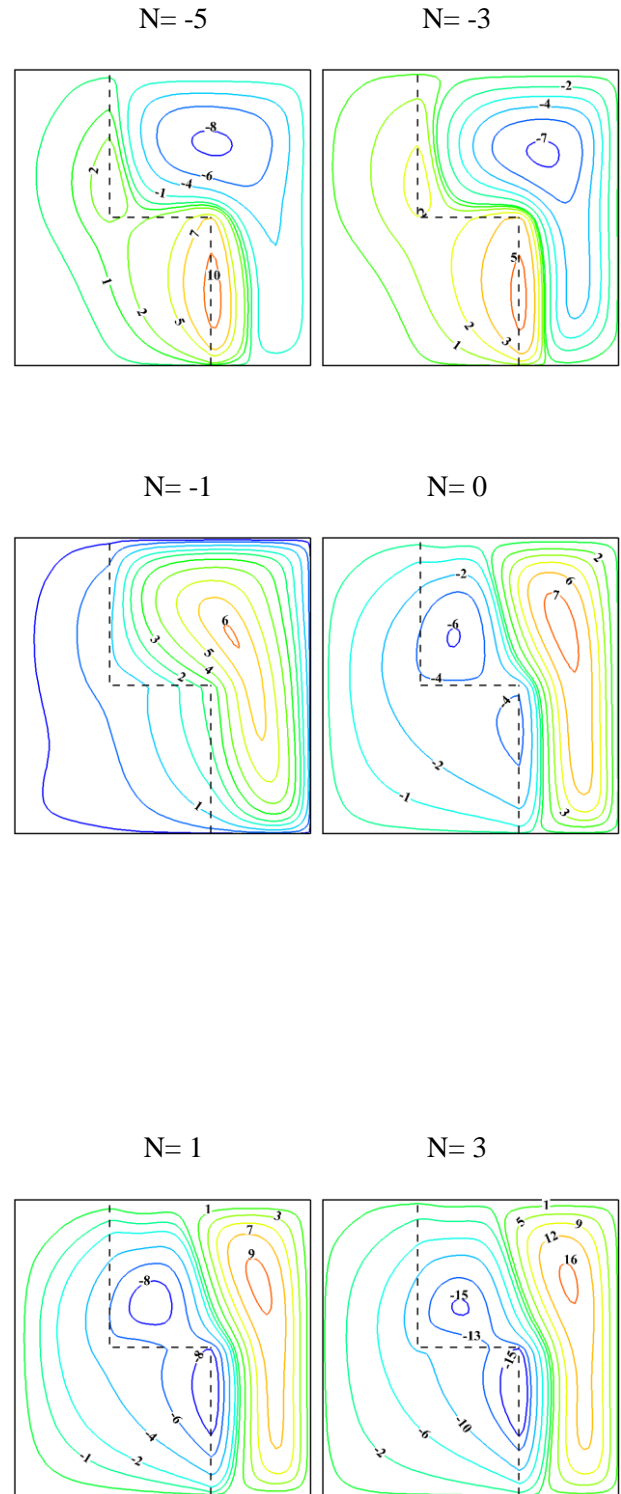


Figure 9. Streamlines for various values of buoyancy ratio N for $\alpha = 15^\circ$.

4.3. Heat and mass transfer parameters

The evolution of heat and mass transfer of the entire porous cavity versus the angle of inclination (α) at different values of buoyancy ratio N is presented in Figures 10 and 11. In general, when the angle of inclination (α) increases clockwise or counterclockwise both Nusselt number and Sherwood number increase for all values of the buoyancy ratio (except $N=-1$) until (α) reaches 75° . When $N=-1$, Nusselt number increases with increasing of the angle of inclination while Sherwood number remaining constant. The same behavior can be seen (Nusselt number and Sherwood number increase) when the buoyancy ratio

increases. The previous results shows that the maximum Nu happens when $\alpha=75^\circ$ and at the same inclination the maximum Sh happens for the opposing flow and neighborhood 45° for the assisting flow. Furthermore, the Nusselt and Sherwood number increase with increasing of the buoyancy ratio N excepting the value $N=-1$ where the minimum of both Nu and Sh happens. The maximum of both Nu and Sh happens when N reaches the maximum value ($N=5$). The increase of the Nusselt and Sherwood numbers is due to the increasing the thermal and solutal buoyancy resulting from the increase of inclination angle (α) or buoyancy ratio N .

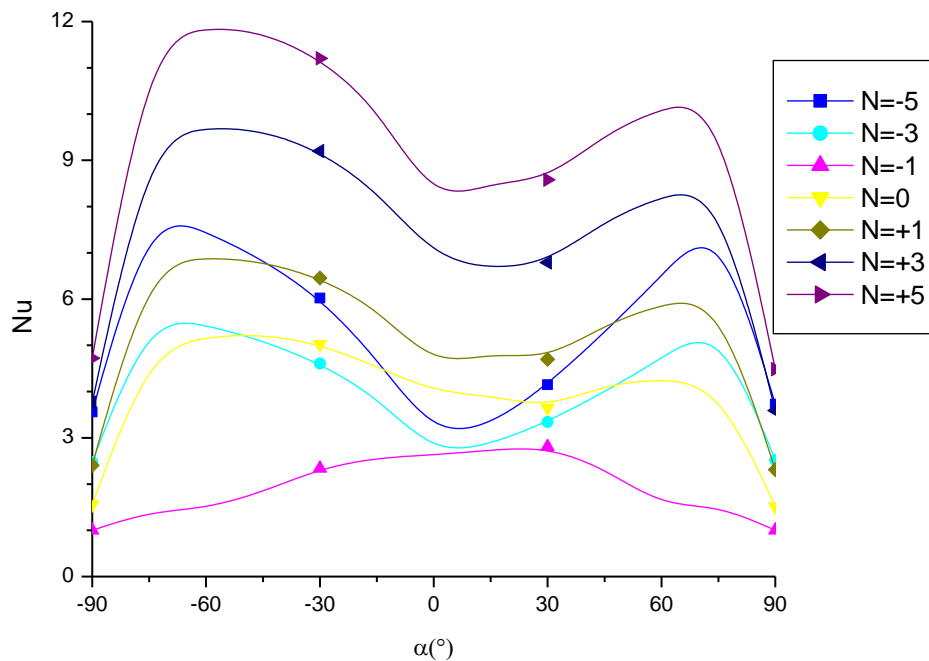


Figure 10. Average Nusselt number with angle of inclination (α) at different values of buoyancy ratio N .

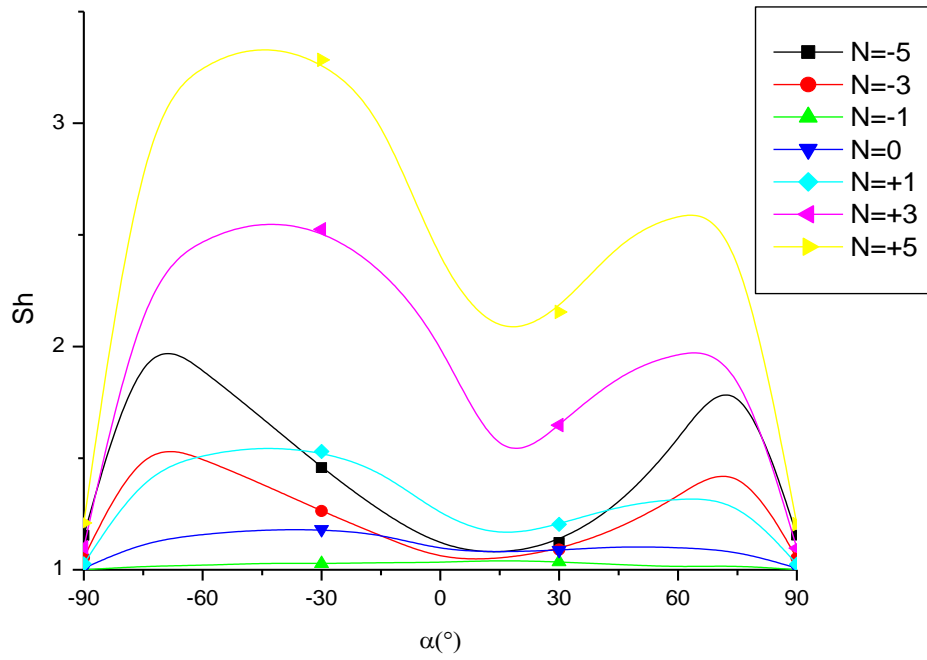


Figure 11. Average Sherwood number with angle of inclination (α) at different values of buoyancy ratio N .

5. Conclusion

Numerical steady of double diffusive natural convection heat and mass transfer generated in an inclined square bi-L-shaped layered porous cavity filled with Newtonian fluid has been investigated. Brinkman-Forchheimer-extended Darcy model has been used to solve the governing equations. A number of relevant results have been presented in this paper for different values of inclination angle of the cavity ($-90^{\circ} \leq \alpha \leq 90^{\circ}$) and the buoyancy ratio ($-5 \leq N \leq 5$), while Rayleigh, Lewis and Prandtl numbers are taken as $5 \cdot 10^6$, 0.1 and 4.5 respectively. The porosity and the Darcy number of the 2 layers are $\epsilon_1=0.6$, $\epsilon_2=0.4$, $Da_1=10^{-5}$ and $Da_2=10^{-4}$. The results showed that; single or multiple cell convection can take place with different tilt angles and buoyancy ratios. In general, the average Nusselt and Sherwood numbers increase when the inclination angle and/or the buoyancy ratio increase. Furthermore, the maximum Nu happens when ($\alpha = -75^{\circ}$) and at the same inclination the maximum Sh happens for the opposing flow and when ($\alpha = -45^{\circ}$) for the assisting flow, and both of them reaches the maximum value when ($N=5$). Work is under way for additional studies incorporating.

Nomenclature

A	aspect ratio, $[=L/H]$
-----	------------------------

a	thermal diffusivity, $m^2 \cdot s^{-1}$
D	solutal diffusivity, $m^2 \cdot s^{-1}$
Da_i	Darcy number of layer i , $[=K_i/H^2]$
g	acceleration due to gravity, $m \cdot s^{-2}$
H	height of the cavity, m
k_i	thermal conductivity of porous layer i , $W \cdot m^{-1} \cdot K^{-1}$
K_i	permeability of layer i , m^2
L	length of the enclosure, m
Le	Lewis number, $[=a/D]$
N	buoyancy ratio, $[=\beta_S(S_h - S_l)/\beta_T(T_h - T_l)]$
Nu	Nusselt number
P	pressure, $kg \cdot m^{-1} \cdot s^{-2}$
P	dimensionless pressure, $[=\epsilon^2 H^2 P / \rho_0 a^2]$
Pr	Prandtl number, $[=\nu/a]$
Ra	Rayleigh number, $[=g\beta_T(T_h - T_l)H^3/\nu a]$

S	dimensional concentration, kg.m^{-3}
S	dimensionless concentration
Sh	average Sherwood number
t	time, s
t	dimensionless time, $[= a.t/H^2]$
T	dimensional temperature, K
T	dimensionless temperature, $[= (T-T_l)/(T_h-T_l)]$
u	velocity components in x direction, m.s^{-1}
u	dimensionless velocity components in x direction $[=H.u/a]$
v	velocity components in y direction, m.s^{-1}
v	dimensionless velocity components in y direction $[=H.v/a]$
x,y	coordinates system, m
x, (y)	dimensionless coordinate system, $[=x(y)/H]$
Greek symbols	
α	inclination angle, $^\circ$
β_s	solubility expansion coefficient, K^{-1}
β_T	thermal expansion coefficient, $(\text{m}^3.\text{kg}^{-1})$
ε_i	porosity of the porous layer i,
ν	kinematic viscosity, $\text{m}^2.\text{s}^{-1}$
ρ	density of fluid, kg.m^{-3}
σ	ratio of specific heats
Subscripts	
h	higher
i	porous layer
l	lower

<i>max</i>	maximum value
------------	---------------

References

- [1] A. Islama, M. Sharif, E. Carlsona. Numerical investigation of double diffusive natural convection of CO₂ in a brine saturated geothermal reservoir. *Geothermics*.48(2013) 101-111.
- [2] T.Nagel, H.Shao, A.Singh, N.Watanabe, C.Roßkopf, M.Linder. Nonequilibriumthermochemical heat storage in porous media: part 1-conceptual model.*Energy*60 (2013) 254-270.
- [3] H. Shao, T. Nagel, C.Roßkopf, M. Linder, A.W€orner, O.Kolditz. Non-equilibrium thermochemical heat storage in porous media: part 2-A 1D computational model for a calcium hydroxidereaction system. *Energy*60 (2013)271-282.
- [4] Y.Liu,H.Wang, Z.Shen, Y.Song. Estimation of CO₂ storage capacity in porous media by using X-ray micro-CT. *Energy Procedia*37(2013) 5201-5208.
- [5] A. Nouri-Borujerdi, SI. Tabatabai. Porous media approach in thermo-hydraulic analysis of high temperature reactors in pressurized/depressurized cool down: an improvement. *ProgNucl Energy*80(2015) 119-127.
- [6] C. Beghein, F. Haghighat, F. Allard, Numerical study of double-diffusive natural convection in a square cavity,*Int J Heat Mass Transf.* 35(1992) 833-846.
- [7] R.W. Schmitt, Double diffusion in oceanography, *Fluid Mech.* 26(1994) 255-285
- [8] J.S. Turner, Double diffusive phenomena, *Fluid Mech.* 6 (1974) 37-56
- [9] S. Ostrach, Natural convection with combined driving forces, *Physicochem. Hydrodyn.* 1(1980) 233-247
- [10] D. Nield, and A. Bejan, *Convection in Porous Media*, 3rd ed. Spinger, New York Inc,2006
- [11] D. B. Ingham, and I. pop, *Transport phenomena in porous media*, 3rd ed. Elsevier, Oxford, 2005
- [12] P. Vadász, *emergingtopics in heat and mass transfer in porous media*. Spinger, New York Inc. 2008
- [13] R. Viskanta, T.L. Bergman, F.P. Incropera, Double diffusive natural convection, in: S. Kakac,W. Aung, R. Viskanta (Eds.), *Natural Convection: Fundamentals and Applications*, Hemisphere, Washington, DC, 1985
- [14] H. Fernando, Buoyancy transfer across a diffusive interface, *J. Fluid Mech.* 209(1989) 1-34.
- [15] T. Makayssi, M. Lamsaadi, M. Naimi, M. Hasnaoui, A. Raji, A. Bahlaoui, Natural double-diffusive convection in a shallow horizontal rectangular cavity uniformly heated and salted from the side and filled with non-Newtonian power-law

- fluids: the cooperating case, *Energy Convers. Manage.* 49 (2008) 2016-2025
- [16] M.A. Teamah, Numerical simulation of double diffusive natural convection in rectangular enclosure in the presences of magnetic field and heat source, *Int. J. Therm. Sci.* 47 (2008) 237-248
- [17] H.S. Harzallah, A. Jbara, K. Slimi, Double-diffusive natural convection in anisotropic porous medium bounded by finite thickness walls: validity of local thermal equilibrium assumption, *Transp. Porous Med.* 103 (2014) 207-231
- [18] Z. Alloui, P. Vasseur, Convection of a binary fluid in a shallow porous cavity heated and salted from the sides, *Computers & Fluids* 81 (2013) 85-94
- [19] R. Nikbakhti, J. Khodakhah, Numerical investigation of double diffusive buoyancy forces induced natural convection in a cavity partially heated and cooled from sidewalls, *Engineering Science and Technology, an International Journal*(2015)
- [20] M.A. Teamah, M. M. KhairatDawood, W.M. El-Maghlany, Double diffusive natural convection in a square cavity with segmental heat sources, *Eur. J. Sci. Res.* 54 (2) (2011) 287-301.
- [21] K. Al-Farhany, A. Turan, Numerical study of double diffusive natural convective heat and mass transfer in an inclined rectangular cavity filled with porous, *International Communications in Heat and Mass Transfer* 39 (2012) 174-181.
- [22] V.J. Bansod, R.K. Jadhav, An integral treatment for combined heat and mass transfer by natural convection along a horizontal surface in a porous medium, *International Journal of Heat and Mass Transfer* 52 (2009) 2802-2806.
- [23] F. Zhao, D. Liu, G. Tang, Natural convection in an enclosure with localized heating and salting from below, *International Journal of Heat and Mass Transfer* 51 (2008) 2889-2904
- [24] A. Latreche, M. Djeddar, Convective heat and solute transfer in Newtonian fluid saturated inclined porous cavity, *International Journal of Physical Research* 2(2) (2014) 78-84.
- [25] Mohamad, R. Bennacer, Natural convection in a confined saturated porous medium with horizontal temperature and vertical solutal gradients, *Int. J. Therm. Sci.*40 (2001) 82-93
- [26] M. Bourich, A. Amahmid, M. Hasnaoui, Double diffusive convection in a porous enclosure submitted to cross gradients of temperature and concentration, *Energy Conversion and Management* 45 (2004) 1655-1670.
- [27] S. Roy, T. Basak, Finite element analysis of natural convection flows in a square cavity with non-uniformly heated wall(s), *Int. J. Eng. Sci.* 43 (2005) 668-680.
- [28] N.Hadidi, Y. Ould-Amer, R. Bennacer, Bi-layered and inclined porous collector: optimum heat and mass transfer. *Energy* 51 (2013) 422-430.
- [29] N.Hadidi, R. Bennacer, Y. Ould-Amer, Two-dimensional thermosolutal natural convective heat and mass transfer in a bi-layered and inclined porous enclosure. *Energy* 93 (2015) 2582-2592.
- [30] AC. Baytas , AF. Baytas, DB. Ingham, I. Pop. Double diffusive natural convection in an enclosure filled with a step type porous layer: non-darcy flow. *Int J Therm Sci.* 48 (2009) 665-673.
- [31] R. Bennacer, H. Beji, A.A. Mohamad, Double diffusive convection in a vertical enclosure insertedwith two saturated porous layers confining a fluid layer, *International Journal of Thermal Sciences* 42 (2003) 141-151.
- [32] S. Patankar, *Numerical Heat Transfer and Fluid flow*, Hemisphere, New York, 1980.
- [33] S.L. Moya, E. Ramos, M. Sen, Numerical study of natural convection in a tilted rectangular porousmaterial. *International Journal of Heat andMass Transfer* 30 (4) (1987) 741-756.
- [34] J.P. Caltagirone, S. Bories, Solutions and stability criteria of natural convective flow in an inclined porous layer. *Journal of Fluid Mechanics* 155 (1985) 267-287.